Searches for direct pair production of supersymmetric top and supersymmetric bottom quarks in $p\bar{p}$ collisions at $\sqrt{s} = 1.96$ TeV

T. Aaltonen,[23] A. Abulencia,[24] J. Adelman,[13] T. Affolder,[10] T. Akimoto,[55] M. G. Albrow,[17] S. Amerio,[43] D. Amidei,[35] A. Anastassov,[52] K. Anikeev,[17] A. Annovi,[19] J. Antos,[14] M. Aoki,[55] G. Apollinari,[17] T. Arisawa,[57] A. Artikov,[15] W. Ashmanskas,[17] A. Attal,[3] A. Aurisano,[53] F. Azfar,[42] P. Azzi-Bacchetta,[43] P. Azzurri,[46] N. Bacchetta,[43] W. Badgett,[17] A. Barbaro-Galtieri,[29] V. E. Barnes,[48] B. A. Barnett,[25] S. Baroiant,[7] V. Bartsch,[31] G. Bauer,[33] P.-H. Beauchemin,[34] F. Bedeschi,[46] S. Behari,[25] G. Bellettini,[46] J. Bellinger,[59] A. Belloni,[33] D. Benjamin,[16] A. Beretvas,[17] J. Beringer,[29] T. Berry,[30] A. Bhatti,[50] M. Binkley,[17] D. Bisello,[43] I. Bizjak,[31] R. E. Blair,[2] C. Blocker,[6] B. Blumenfeld,[25] A. Bocci,[16] A. Bodek,[49] V. Boisvert,[49] G. Bolla,[48] A. Bolshov,[33] D. Bortoletto,[48] J. Boudreau,[47] A. Boveia,[10] B. Brau,[10] L. Brigliadori,[5] C. Bromberg,[36] E. Brubaker,[13] J. Budagov,[15] H. S. Budd,[49] S. Budd,[24] K. Burkett,[17] G. Busetto,[43] P. Bussey,[21] A. Buzatu,[34] K. L. Byrum,[2] S. Cabrera,[16,q] M. Campanelli,[20] M. Campbell,[35] F. Canelli,[17] A. Canepa,[45] S. Carillo,[18,i] D. Carlsmith,[59] R. Carosi,[46] S. Carron,[34] B. Casal,[11] M. Casarsa,[54] A. Castro,[5] P. Catastini,[46] D. Cauz,[54] M. Cavalli-Sforza,[3] A. Cerri,[29] L. Cerrito,[31,m] S. H. Chang,[28] Y. C. Chen,[1] M. Chertok,[7] G. Chiarelli,[46] G. Chlachidze,[17] F. Chlebana,[17] I. Cho,[28] K. Cho,[28] D. Chokheli,[15] J. P. Chou,[22] G. Choudalakis,[33] S. H. Chuang,[52] K. Chung,[12] W. H. Chung,[59] Y. S. Chung,[49] M. Cilijak,[46] C. I. Ciobanu,[24] M. A. Ciocci,[46] A. Clark,[20] D. Clark,[6] M. Coca,[16] G. Compostella,[43] M. E. Convery,[50] J. Conway,[7] B. Cooper,[31] K. Copic,[35] M. Cordelli,[19] G. Cortiana,[43] F. Crescioli,[46] C. Cuenca Almenar,[7,q] J. Cuevas,[11,l] R. Culbertson,[17] J. C. Cully,[35] S. DaRonco,[43] M. Datta,[17] S. D'Auria,[21] T. Davies,[21] D. Dagenhart,[17] P. de Barbaro,[49] S. De Cecco,[51] A. Deisher,[29] G. De Lentdecker,[49,c] G. De Lorenzo,[3] M. Dell'Orso,[46] F. Delli Paoli,[43] L. Demortier,[50] J. Deng,[16] M. Deninno,[5] D. De Pedis,[51] P. F. Derwent,[17] G. P. Di Giovanni,[44] C. Dionisi,[51] B. Di Ruzza,[54] J. R. Dittmann,[4] M. D'Onofrio,[3] C. Dörr,[26] S. Donati,[46] P. Dong,[8] J. Donini,[43] T. Dorigo,[43] S. Dube,[52] J. Efron,[39] R. Erbacher,[7] D. Errede,[24] S. Errede,[24] R. Eusebi,[17] H. C. Fang,[29] S. Farrington,[30] I. Fedorko,[46] W. T. Fedorko,[13] R. G. Feild,[60] M. Feindt,[26] J. P. Fernandez,[32] R. Field,[18] G. Flanagan,[48] R. Forrest,[7] S. Forrester,[7] M. Franklin,[22] J. C. Freeman,[29] I. Furic,[13] M. Gallinaro,[50] J. Galyardt,[12] J. E. Garcia,[46] F. Garberson,[10] A. F. Garfinkel,[48] C. Gay,[60] H. Gerberich,[24] D. Gerdes,[35] S. Giagu,[51] P. Giannetti,[46] K. Gibson,[47] J. L. Gimmell,[49] C. Ginsburg,[17] N. Giokaris,[15,a] M. Giordani,[54] P. Giromini,[19] M. Giunta,[46] G. Giurgiu,[25] V. Glagolev,[15] D. Glenzinski,[17] M. Gold,[37] N. Goldschmidt,[18] J. Goldstein,[42,b] A. Golossanov,[17] G. Gomez,[11] G. Gomez-Ceballos,[33] M. Goncharov,[53] O. González,[32] I. Gorelov,[37] A. T. Goshaw,[16] K. Goulianos,[50] A. Gresele,[43] S. Grinstein,[22] C. Grosso-Pilcher,[13] R. C. Group,[17] U. Grundler,[24] J. Guimaraes da Costa,[22] Z. Gunay-Unalan,[36] C. Haber,[29] K. Hahn,[33] S. R. Hahn,[17] E. Halkiadakis,[52] A. Hamilton,[20] B.-Y. Han,[49] J. Y. Han,[49] R. Handler,[59] F. Happacher,[19] K. Hara,[55] D. Hare,[52] M. Hare,[56] S. Harper,[42] R. F. Harr,[58] R. M. Harris,[17] M. Hartz,[47] K. Hatakeyama,[50] J. Hauser,[8] C. Hays,[42] M. Heck,[26] A. Heijboer,[45] B. Heinemann,[29] J. Heinrich,[45] C. Henderson,[33] M. Herndon,[59] J. Heuser,[26] D. Hidas,[16] C. S. Hill,[10,b] D. Hirschbuehl,[26] A. Hocker,[17] A. Holloway,[22] S. Hou,[1] M. Houlden,[30] S.-C. Hsu,[9] B. T. Huffman,[42] R. E. Hughes,[39] U. Husemann,[60] J. Huston,[36] J. Incandela,[10] G. Introzzi,[46] M. Iori,[51] A. Ivanov,[7] B. Iyutin,[33] E. James,[17] D. Jang,[52] B. Jayatilaka,[16] D. Jeans,[51] E. J. Jeon,[28] S. Jindariani,[18] W. Johnson,[7] M. Jones,[48] K. K. Joo,[28] S. Y. Jun,[12] J. E. Jung,[28] T. R. Junk,[24] T. Kamon,[53] P. E. Karchin,[58] Y. Kato,[41] Y. Kemp,[26] R. Kephart,[17] U. Kerzel,[26] V. Khotilovich,[53] B. Kilminster,[39] D. H. Kim,[28] H. S. Kim,[28] J. E. Kim,[28] M. J. Kim,[17] S. B. Kim,[28] S. H. Kim,[55] Y. K. Kim,[13] N. Kimura,[55] L. Kirsch,[6] S. Klimenko,[18] M. Klute,[33] B. Knuteson,[33] B. R. Ko,[16] K. Kondo,[57] D. J. Kong,[28] J. Konigsberg,[18] A. Korytov,[18] A. V. Kotwal,[16] A. C. Kraan,[45] J. Kraus,[24] M. Kreps,[26] J. Kroll,[45] N. Krumnack,[4] M. Kruse,[16] V. Krutelyov,[10] T. Kubo,[55] S. E. Kuhlmann,[2] T. Kuhr,[26] N. P. Kulkarni,[58] Y. Kusakabe,[57] S. Kwang,[13] A. T. Laasanen,[48] S. Lai,[34] S. Lami,[46] S. Lammel,[17] M. Lancaster,[31] R. L. Lander,[7] K. Lannon,[39] A. Lath,[52] G. Latino,[46] I. Lazzizzera,[43] T. LeCompte,[2] J. Lee,[49] J. Lee,[28] Y. J. Lee,[28] S. W. Lee,[53,o] R. Lefèvre,[20] N. Leonardo,[33] S. Leone,[46] S. Levy,[13] J. D. Lewis,[17] C. Lin,[60] C. S. Lin,[17] M. Lindgren,[17] E. Lipeles,[9] A. Lister,[7] D. O. Litvintsev,[17] T. Liu,[17] N. S. Lockyer,[45] A. Loginov,[60] M. Loreti,[43] R.-S. Lu,[1] D. Lucchesi,[43] P. Lujan,[29] P. Lukens,[17] G. Lungu,[18] L. Lyons,[42] J. Lys,[29] R. Lysak,[14] E. Lytken,[48] P. Mack,[26] D. MacQueen,[34] R. Madrak,[17] K. Maeshima,[17] K. Makhoul,[33] T. Maki,[23] P. Maksimovic,[25] S. Malde,[42] S. Malik,[31] G. Manca,[30] A. Manousakis,[15,a] F. Margaroli,[5] R. Marginean,[17] C. Marino,[26] C. P. Marino,[24] A. Martin,[60] M. Martin,[25] V. Martin,[21,g] M. Martínez,[3] R. Martínez-Ballarín,[32] T. Maruyama,[55] P. Mastrandrea,[51] T. Masubuchi,[55] H. Matsunaga,[55] M. E. Mattson,[58] R. Mazini,[34] P. Mazzanti,[5] K. S. McFarland,[49] P. McIntyre,[53] R. McNulty,[30,f] A. Mehta,[30] P. Mehtala,[23] S. Menzemer,[11,h] A. Menzione,[46] P. Merkel,[48] C. Mesropian,[50] A. Messina,[36] T. Miao,[17] N. Miladinovic,[6] J. Miles,[33] R. Miller,[36] C. Mills,[10] M. Milnik,[26] A. Mitra,[1] G. Mitselmakher,[18] A. Miyamoto,[27] S. Moed,[20] N. Moggi,[5] B. Mohr,[8] C. S. Moon,[28] R. Moore,[17] M. Morello,[46] P. Movilla Fernandez,[29] J. Mülmenstädt,[29] A. Mukherjee,[17] Th. Muller,[26]

R. Mumford,[25] P. Murat,[17] M. Mussini,[5] J. Nachtman,[17] A. Nagano,[55] J. Naganoma,[57] K. Nakamura,[55] I. Nakano,[40] A. Napier,[56] V. Necula,[16] C. Neu,[45] M. S. Neubauer,[9] J. Nielsen,[29,n] L. Nodulman,[2] O. Norniella,[3] E. Nurse,[31] S. H. Oh,[16] Y. D. Oh,[28] I. Oksuzian,[18] T. Okusawa,[41] R. Oldeman,[30] R. Orava,[23] K. Osterberg,[23] C. Pagliarone,[46] E. Palencia,[11] V. Papadimitriou,[17] A. Papaikonomou,[26] A. A. Paramonov,[13] B. Parks,[39] S. Pashapour,[34] J. Patrick,[17] G. Pauletta,[54] M. Paulini,[12] C. Paus,[33] D. E. Pellett,[7] A. Penzo,[54] T. J. Phillips,[16] G. Piacentino,[46] J. Piedra,[44] L. Pinera,[18] K. Pitts,[24] C. Plager,[8] L. Pondrom,[59] X. Portell,[3] O. Poukhov,[15] N. Pounder,[42] F. Prakoshyn,[15] A. Pronko,[17] J. Proudfoot,[2] F. Ptohos,[19,e] G. Punzi,[46] J. Pursley,[25] J. Rademacker,[42,b] A. Rahaman,[47] V. Ramakrishnan,[59] N. Ranjan,[48] I. Redondo,[32] B. Reisert,[17] V. Rekovic,[37] P. Renton,[42] M. Rescigno,[51] S. Richter,[26] F. Rimondi,[5] L. Ristori,[46] A. Robson,[21] T. Rodrigo,[11] E. Rogers,[24] S. Rolli,[56] R. Roser,[17] M. Rossi,[54] R. Rossin,[10] P. Roy,[34] A. Ruiz,[11] J. Russ,[12] V. Rusu,[13] H. Saarikko,[23] A. Safonov,[53] W. K. Sakumoto,[49] G. Salamanna,[51] O. Saltó,[3] L. Santi,[54] S. Sarkar,[51] L. Sartori,[46] K. Sato,[17] P. Savard,[34] A. Savoy-Navarro,[44] T. Scheidle,[26] P. Schlabach,[17] E. E. Schmidt,[17] M. P. Schmidt,[60] M. Schmitt,[38] T. Schwarz,[7] L. Scodellaro,[11] A. L. Scott,[10] A. Scribano,[46] F. Scuri,[46] A. Sedov,[48] S. Seidel,[37] Y. Seiya,[41] A. Semenov,[15] L. Sexton-Kennedy,[17] A. Sfyrla,[20] S. Z. Shalhout,[58] M. D. Shapiro,[29] T. Shears,[30] P. F. Shepard,[47] D. Sherman,[22] M. Shimojima,[55,k] M. Shochet,[13] Y. Shon,[59] I. Shreyber,[20] A. Sidoti,[46] P. Sinervo,[34] A. Sisakyan,[15] A. J. Slaughter,[17] J. Slaunwhite,[39] K. Sliwa,[56] J. R. Smith,[7] F. D. Snider,[17] R. Snihur,[34] M. Soderberg,[35] A. Soha,[7] S. Somalwar,[52] V. Sorin,[36] J. Spalding,[17] F. Spinella,[46] T. Spreitzer,[34] P. Squillacioti,[46] M. Stanitzki,[60] A. Staveris-Polykalas,[46] R. St. Denis,[21] B. Stelzer,[8] O. Stelzer-Chilton,[42] D. Stentz,[38] J. Strologas,[37] D. Stuart,[10] J. S. Suh,[28] A. Sukhanov,[18] H. Sun,[56] I. Suslov,[15] T. Suzuki,[55] A. Taffard,[24,p] R. Takashima,[40] Y. Takeuchi,[55] R. Tanaka,[40] M. Tecchio,[35] P. K. Teng,[1] K. Terashi,[50] J. Thom,[17,d] A. S. Thompson,[21] E. Thomson,[45] P. Tipton,[60] V. Tiwari,[12] S. Tkaczyk,[17] D. Toback,[53] S. Tokar,[14] K. Tollefson,[36] T. Tomura,[55] D. Tonelli,[46] S. Torre,[19] D. Torretta,[17] S. Tourneur,[44] W. Trischuk,[34] S. Tsuno,[40] Y. Tu,[45] N. Turini,[46] F. Ukegawa,[55] S. Uozumi,[55] S. Vallecorsa,[20] N. van Remortel,[23] A. Varganov,[35] E. Vataga,[37] F. Vazquez,[18,i] G. Velev,[17] C. Vellidis,[46,a] G. Veramendi,[24] V. Veszpremi,[48] M. Vidal,[32] R. Vidal,[17] I. Vila,[11] R. Vilar,[11] T. Vine,[31] M. Vogel,[37] I. Vollrath,[34] I. Volobouev,[29,o] G. Volpi,[46] F. Würthwein,[9] P. Wagner,[53] R. G. Wagner,[2] R. L. Wagner,[17] J. Wagner,[26] W. Wagner,[26] R. Wallny,[8] S. M. Wang,[1] A. Warburton,[34] D. Waters,[31] M. Weinberger,[53] W. C. Wester III,[17] B. Whitehouse,[56] D. Whiteson,[45,p] A. B. Wicklund,[2] E. Wicklund,[17] G. Williams,[34] H. H. Williams,[45] P. Wilson,[17] B. L. Winer,[39] P. Wittich,[17,d] S. Wolbers,[17] C. Wolfe,[13] T. Wright,[35] X. Wu,[20] S. M. Wynne,[30] A. Yagil,[9] K. Yamamoto,[41] J. Yamaoka,[52] T. Yamashita,[40] C. Yang,[60] U. K. Yang,[13,j] Y. C. Yang,[28] W. M. Yao,[29] G. P. Yeh,[17] J. Yoh,[17] K. Yorita,[13] T. Yoshida,[41] G. B. Yu,[49] I. Yu,[28] S. S. Yu,[17] J. C. Yun,[17] L. Zanello,[51] A. Zanetti,[54] I. Zaw,[22] X. Zhang,[24] J. Zhou,[52] and S. Zucchelli[5]

(CDF Collaboration)[a]

[1]*Institute of Physics, Academia Sinica, Taipei, Taiwan 11529, Republic of China*
[2]*Argonne National Laboratory, Argonne, Illinois 60439, USA*
[3]*Institut de Fisica d'Altes Energies, Universitat Autonoma de Barcelona, E-08193, Bellaterra (Barcelona), Spain*
[4]*Baylor University, Waco, Texas 76798, USA*
[5]*Istituto Nazionale di Fisica Nucleare, University of Bologna, I-40127 Bologna, Italy*
[6]*Brandeis University, Waltham, Massachusetts 02254, USA*
[7]*University of California, Davis, Davis, California 95616, USA*
[8]*University of California, Los Angeles, Los Angeles, California 90024, USA*
[9]*University of California, San Diego, La Jolla, California 92093, USA*
[10]*University of California, Santa Barbara, Santa Barbara, California 93106, USA*
[11]*Instituto de Fisica de Cantabria, CSIC-University of Cantabria, 39005 Santander, Spain*
[12]*Carnegie Mellon University, Pittsburgh, Pennsylvania 15213, USA*
[13]*Enrico Fermi Institute, University of Chicago, Chicago, Illinois 60637, USA*
[14]*Comenius University, 842 48 Bratislava, Slovakia;*
Institute of Experimental Physics, 040 01 Kosice, Slovakia
[15]*Joint Institute for Nuclear Research, RU-141980 Dubna, Russia*
[16]*Duke University, Durham, North Carolina 27708, USA*
[17]*Fermi National Accelerator Laboratory, Batavia, Illinois 60510, USA*
[18]*University of Florida, Gainesville, Florida 32611, USA*
[19]*Laboratori Nazionali di Frascati, Istituto Nazionale di Fisica Nucleare, I-00044 Frascati, Italy*
[20]*University of Geneva, CH-1211 Geneva 4, Switzerland*
[21]*Glasgow University, Glasgow G12 8QQ, United Kingdom*
[22]*Harvard University, Cambridge, Massachusetts 02138, USA*

[23]*Division of High Energy Physics, Department of Physics, University of Helsinki and Helsinki Institute of Physics, FIN-00014, Helsinki, Finland*
[24]*University of Illinois, Urbana, Illinois 61801, USA*
[25]*The Johns Hopkins University, Baltimore, Maryland 21218, USA*
[26]*Institut für Experimentelle Kernphysik, Universität Karlsruhe, 76128 Karlsruhe, Germany*
[27]*High Energy Accelerator Research Organization (KEK), Tsukuba, Ibaraki 305, Japan*
[28]*Center for High Energy Physics: Kyungpook National University, Taegu 702-701, Korea; Seoul National University, Seoul 151-742, Korea; SungKyunKwan University, Suwon 440-746, Korea*
[29]*Ernest Orlando Lawrence Berkeley National Laboratory, Berkeley, California 94720, USA*
[30]*University of Liverpool, Liverpool L69 7ZE, United Kingdom*
[31]*University College London, London WC1E 6BT, United Kingdom*
[32]*Centro de Investigaciones Energeticas Medioambientales y Tecnologicas, E-28040 Madrid, Spain*
[33]*Massachusetts Institute of Technology, Cambridge, Massachusetts 02139, USA*
[34]*Institute of Particle Physics: McGill University, Montréal, Canada H3A 2T8; and University of Toronto, Toronto, Canada M5S 1A7*
[35]*University of Michigan, Ann Arbor, Michigan 48109, USA*
[36]*Michigan State University, East Lansing, Michigan 48824, USA*
[37]*University of New Mexico, Albuquerque, New Mexico 87131, USA*
[38]*Northwestern University, Evanston, Illinois 60208, USA*
[39]*The Ohio State University, Columbus, Ohio 43210, USA*
[40]*Okayama University, Okayama 700-8530, Japan*
[41]*Osaka City University, Osaka 588, Japan*
[42]*University of Oxford, Oxford OX1 3RH, United Kingdom*
[43]*University of Padova, Istituto Nazionale di Fisica Nucleare, Sezione di Padova-Trento, I-35131 Padova, Italy*
[44]*LPNHE, Universite Pierre et Marie Curie/IN2P3-CNRS, UMR7585, Paris, F-75252 France*
[45]*University of Pennsylvania, Philadelphia, Pennsylvania 19104, USA*
[46]*Istituto Nazionale di Fisica Nucleare Pisa, Universities of Pisa, Siena and Scuola Normale Superiore, I-56127 Pisa, Italy*
[47]*University of Pittsburgh, Pittsburgh, Pennsylvania 15260, USA*
[48]*Purdue University, West Lafayette, Indiana 47907, USA*
[49]*University of Rochester, Rochester, New York 14627, USA*
[50]*The Rockefeller University, New York, New York 10021, USA*
[51]*Istituto Nazionale di Fisica Nucleare, Sezione di Roma 1, University of Rome "La Sapienza," I-00185 Roma, Italy*
[52]*Rutgers University, Piscataway, New Jersey 08855, USA*
[53]*Texas A&M University, College Station, Texas 77843, USA*
[54]*Istituto Nazionale di Fisica Nucleare, University of Trieste/Udine, Italy*
[55]*University of Tsukuba, Tsukuba, Ibaraki 305, Japan*
[56]*Tufts University, Medford, Massachusetts 02155, USA*
[57]*Waseda University, Tokyo 169, Japan*

[a]Visiting scientist from University of Athens, 15784 Athens, Greece.
[b]Visiting scientist from University of Bristol, Bristol BS8 1TL, United Kingdom.
[c]Visiting scientist from University Libre de Bruxelles, B-1050 Brussels, Belgium.
[d]Visiting scientist from Cornell University, Ithaca, NY 14853, USA.
[e]Visiting scientist from University of Cyprus, Nicosia CY-1678, Cyprus.
[f]Visiting scientist from University College Dublin, Dublin 4, Ireland.
[g]Visiting scientist from University of Edinburgh, Edinburgh EH9 3JZ, United Kingdom.
[h]Visiting scientist from University of Heidelberg, D-69120 Heidelberg, Germany.
[i]Visiting scientist from Universidad Iberoamericana, Mexico D.F., Mexico.
[j]Visiting scientist from University of Manchester, Manchester M13 9PL, England.
[k]Visiting scientist from Nagasaki Institute of Applied Science, Nagasaki, Japan.
[l]Visiting scientist from University de Oviedo, E-33007 Oviedo, Spain.
[m]Visiting scientist from University of London, Queen Mary College, London, E1 4NS, England.
[n]Visiting scientist from University of California, Santa Cruz, Santa Cruz, CA 95064, USA.
[o]Visiting scientist from Texas Tech University, Lubbock, TX 79409, USA.
[p]Visiting scientist from University of California, Irvine, Irvine, CA 92697, USA.
[q]Visiting scientist from IFIC(CSIC-Universitat de Valencia), 46071 Valencia, Spain.

[58]*Wayne State University, Detroit, Michigan 48201, USA*
[59]*University of Wisconsin, Madison, Wisconsin 53706, USA*
[60]*Yale University, New Haven, Connecticut 06520, USA*
(Received 17 July 2007; published 25 October 2007)

We search for direct pair production of supersymmetric top quarks and supersymmetric bottom quarks in proton-antiproton collisions at $\sqrt{s} = 1.96$ TeV, using 295 pb^{-1} of data recorded by the Collider Detector at Fermilab (CDF II) experiment. The supersymmetric top (supersymmetric bottom) quarks are selected by reconstructing their decay into a charm (bottom) quark and a neutralino, which is assumed to be the lightest supersymmetric particle. The signature of such processes is two energetic heavy-flavor jets and missing transverse energy. The number of events that pass our selection for each search process is consistent with the expected standard model background. By comparing our results to the theoretical production cross sections of the supersymmetric top and supersymmetric bottom quarks in the minimal supersymmetric standard model, we exclude, at a 95% confidence level in the frame of that model, a supersymmetric top quark mass up to 132 GeV/c^2 for a neutralino mass of 48 GeV/c^2, and a supersymmetric bottom quark mass up to 193 GeV/c^2 for a neutralino mass of 40 GeV/c^2.

DOI: 10.1103/PhysRevD.76.072010 PACS numbers: 12.60.Jv, 13.85.Rm, 14.80.Ly

I. INTRODUCTION

Supersymmetry (SUSY) is an extension of the standard model (SM) of particle physics that overcomes some of the theoretical problems in the SM by introducing a new degree of freedom [1]. In this model a bosonic supersymmetric partner is assigned to every SM fermion helicity state, and a fermionic superpartner to every SM boson. Thus, the SM quark helicity states q_L and q_R acquire scalar partners $\tilde{q}_L$ and $\tilde{q}_R$. The mass eigenstates of each supersymmetric quark (squark) can be a mixture of their weak eigenstates, quantified by a mixing angle θ. The difference in the mass eigenvalues depends on several factors. In the case of the supersymmetric top quark (stop), due to the large top quark mass and the large value of its Yukawa coupling constant (Higgs-to-top coupling), there can be a significant difference in the mass between the two mass eigenstates $\tilde{t}_1$ and $\tilde{t}_2$. In the case of the supersymmetric bottom quark (sbottom), a large mass difference between the two mass eigenstates $\tilde{b}_1$ and $\tilde{b}_2$ can occur if the ratio of the vacuum expectation values of the two Higgs fields expected in SUSY is large [2]. In both cases it is likely that the less massive stop ($\tilde{t}_1$) and sbottom ($\tilde{b}_1$) could be lighter than the first two generations of supersymmetric quarks. In fact the $\tilde{t}_1$ could be lighter than the top quark if the top Yukawa coupling strength or the stop mixing is strong enough. The requirement of a light stop is also a feature of many baryogenesis models [3].

In this paper, we describe two analyses searching for stop and sbottom production at the Tevatron using a data sample of 295 pb^{-1} integrated luminosity collected with the CDF II detector. Both analyses are performed within the R-parity [4] conserving minimal supersymmetric standard model framework. A consequence of R-parity conservation is that all SUSY particles are pair produced, and the lightest SUSY particle (LSP) is stable. If the LSP interacts weakly it is a good candidate for cold dark matter and it escapes our detection.

At the Tevatron, stop and sbottom are expected to be produced in pairs mainly via gg fusion and $q\bar{q}$ annihilation, as shown in Fig. 1. At leading order, their production cross sections depend essentially only on their masses. For a center-of-mass energy of 1.96 TeV, the next-to-leading-order (NLO) cross section, calculated with PROSPINO [5], ranges from 50.3 pb to 0.25 pb for stop and sbottom masses from 80 GeV/c^2 to 200 GeV/c^2. In the calculation, the renormalization and factorization scales are set to the mass of stop or sbottom ($Q_{\rm rf} = m_{\tilde{t}_1,\tilde{b}_1}$), and the parton distribution functions (PDFs) are from CTEQ6M [6].

The stop and sbottom can decay in many channels, depending on the mass difference between stop/sbottom and other SUSY and SM particles. Here we consider the SUSY parameter space where the stop and sbottom are relatively light. In the case of stop, the flavor changing loop decay $\tilde{t}_1 \rightarrow c\tilde{\chi}_1^0$ dominates if $m_{\tilde{t}_1} > m_c + m_{\tilde{\chi}_1^0}$, but $m_{\tilde{t}_1} < m_b + m_{\tilde{\chi}_1^\pm}$ and $m_{\tilde{t}_1} < m_W + m_b + m_{\tilde{\chi}_1^0}$. In the sbottom search, the $\tilde{b}_1 \rightarrow b\tilde{\chi}_1^0$ is the only relevant decay if $m_{\tilde{b}_1} > m_b + m_{\tilde{\chi}_1^0}$, but $m_{\tilde{b}_1} < m_b + m_{\tilde{\chi}_2^0}$ and $m_{\tilde{b}_1} < m_t + m_{\tilde{\chi}_1^\pm}$. The neutralinos ($\tilde{\chi}_{1,2,3,4}^0$) and the charginos ($\tilde{\chi}_{1,2}^\pm$) are the SUSY partners of the electroweak bosons and are labeled in order of increasing mass. Therefore, we search for the processes $p\bar{p} \rightarrow \tilde{t}_1\bar{\tilde{t}}_1 \rightarrow (c\tilde{\chi}_1^0)(\bar{c}\tilde{\chi}_1^0)$, and $p\bar{p} \rightarrow \tilde{b}_1\bar{\tilde{b}}_1 \rightarrow (b\tilde{\chi}_1^0)(\bar{b}\tilde{\chi}_1^0)$, as shown in Fig. 2. We assume $\tilde{\chi}_1^0$ is the LSP. Thus, the experimental signature for stop and sbottom pair production processes is a pair of acollinear heavy-flavor jets (i.e. b and c jets), and large missing transverse energy ($\not\!\!E_T$) coming from the escaping LSPs. The searches assume that both stop and sbottom decay very close to the interaction point. For $m_{\tilde{t}_1} = 100$ GeV/c^2 ($m_{\tilde{b}_1} = 160$ GeV/c^2) and $m_{\tilde{\chi}_1^0} = 60$ GeV/c^2, the expected lifetime of stop (sbottom) with only the decay $\tilde{t}_1 \rightarrow c\tilde{\chi}_1^0$ ($\tilde{b}_1 \rightarrow b\tilde{\chi}_1^0$) is of the order of 10^{-15} (10^{-23}) seconds which corresponds to a natural decay length of 0.3 μm (3×10^{-9} μm) [7,8].

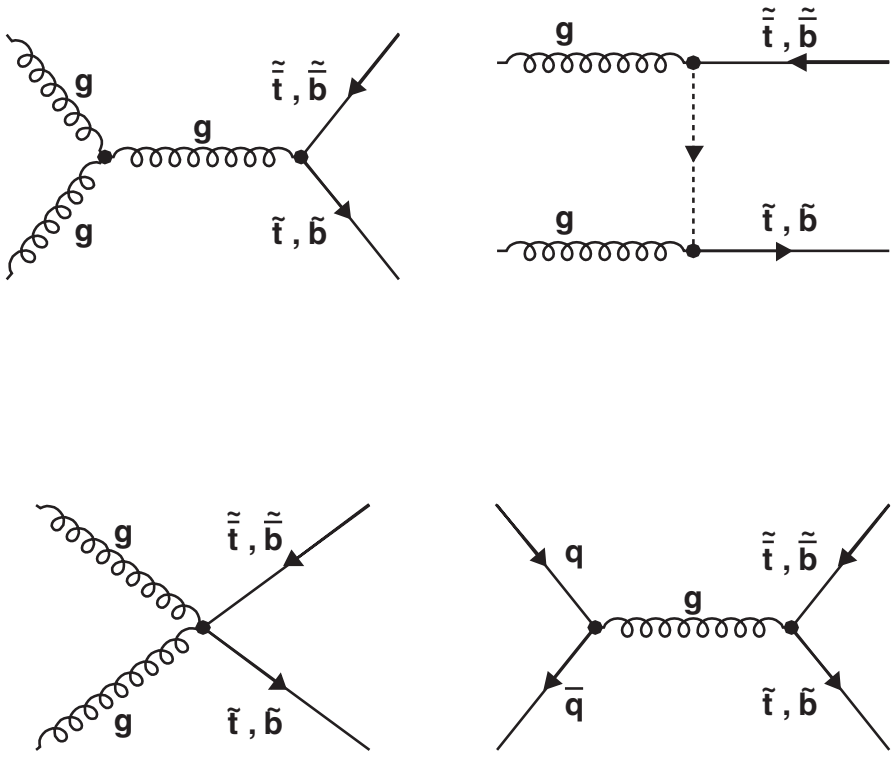

FIG. 1. Leading-order Feynman diagrams for pair production of stop and sbottom at the Tevatron.

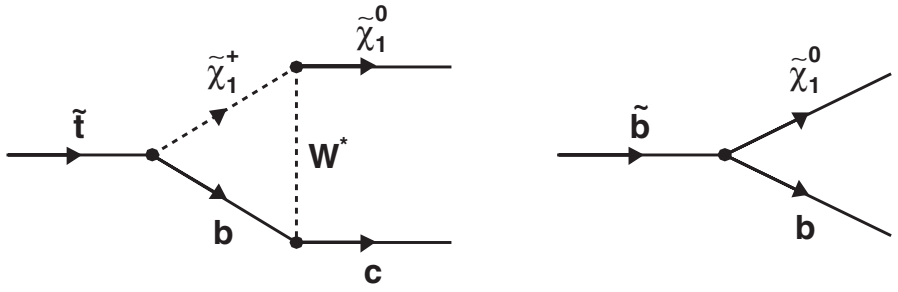

FIG. 2. The decay channels of stop and sbottom considered in this paper.

Previous searches for stop and sbottom have been performed at CERN LEP and at the Tevatron [9–17]. For the search topology studied in the present analysis, LEP excludes stop (sbottom) masses smaller than $\approx 100\ \mathrm{GeV}/c^2$ ($\approx 100\ \mathrm{GeV}/c^2$), independent of the difference between stop (sbottom) and neutralino $\tilde{\chi}_1^0$ masses [9]. Recent results from the D0 Collaboration in the same topology [16,17], based on Run II data, have extended Tevatron's Run I reach [10,11] by excluding stop masses up to $\sim 133\ \mathrm{GeV}/c^2$, and sbottom masses up to $\sim 220\ \mathrm{GeV}/c^2$. These results are also shown in Figs. 4 and 5 of this paper.

II. THE DETECTOR AND DATA SAMPLE

CDF II is a general-purpose detector that is described in detail elsewhere [18]. The components relevant to this analysis are briefly described here. The charged-particle tracking system is closest to the beam pipe, and consists of multiple layers of silicon microstrip detectors, which cover a pseudorapidity region $|\eta| < 2$, and a large open-cell drift chamber covering the pseudorapidity region $|\eta| < 1$ [19–21]. The silicon microstrips of the silicon detectors have a pitch of 25 to 65 μm, depending on the layer, thus allowing a precise measurement of a track's impact parameter with respect to the primary vertex. The tracking system is enclosed in a superconducting solenoid, which in turn is surrounded by calorimeters. The calorimeter system [22] is organized into electromagnetic and hadronic sections segmented in projective tower geometry, and covers the region $|\eta| < 3.6$. The electromagnetic calorimeters use lead-scintillator sampling, whereas the hadron calorimeters use iron-scintillator sampling construction. The transverse

energy resolution of the electromagnetic calorimeters is $\sigma(E_T)/E_T = \frac{13.5\%}{\sqrt{E_T\ (\mathrm{GeV})}} \oplus 2\%$ for the central region ($|\eta| < 1$), and $\sigma(E)/E = \frac{16\%}{\sqrt{E\ (\mathrm{GeV})}} \oplus 1\%$ for the forward region ($|\eta| > 1$). The transverse energy resolution of the hadronic calorimeters is $\sigma(E_T)/E_T = \frac{75\%}{\sqrt{E_T\ (\mathrm{GeV})}} \oplus 3\%$ for the central region, and $\sigma(E)/E = \frac{80\%}{\sqrt{E\ (\mathrm{GeV})}} \oplus 5\%$ for the forward region. The present analysis exploits the information of the central muon system, which is located outside of the calorimeter and covers the range $|\eta| < 1$.

The data sample for this analysis was collected using a $\not\!\!E_T$ + jets trigger, which is implemented in three levels of online event selection. The $\not\!\!E_T$ is defined as the energy imbalance in the plane transverse to the beam direction [21], and a jet is defined as a localized energy deposition in the calorimeter. In the first and second levels of the trigger, $\not\!\!E_T$ is required to be greater than 25 GeV and is calculated by summing over calorimeter trigger towers with transverse energies above 1 GeV. In the second level there must be at least two jets with $E_T > 10$ GeV. In the third level, $\not\!\!E_T$ is recalculated using the full calorimeter segmentation with a tower energy threshold of 100 MeV and is required to be greater than 35 GeV.

In the offline processing, jets are reconstructed from the calorimeter towers using a cone algorithm with fixed radius $\Delta R \equiv \sqrt{\Delta\eta^2 + \Delta\phi^2} = 0.4$ in $\eta - \phi$ space [23]. The jet E_T measurements and $\not\!\!E_T$ are corrected for detector effects [24].

A fraction of events passing the trigger is not from $p\bar{p}$ collisions, but from beam halo and cosmic ray sources. To remove these events we examine the event electromagnetic fraction F_{em} and charged fraction F_{ch}. The F_{em} is the ratio of the energy measured by the electromagnetic calorimeter to the total energy contained in jets of cone radius $\Delta R = 0.4$ with $E_T > 10$ GeV and $|\eta| < 3.6$. The F_{ch} is the fraction of the jet energy carried by measured charged-particle tracks ($p_T > 0.5$ GeV/c) averaged over jets with $|\eta| < 0.9$. The beam halo travels parallel to the beam axis and deposits most of its energy in the electromagnetic section of the calorimeter or in the hadronic section. By requiring $F_{\mathrm{em}} > 0.1$ we reject events which contain little energy in the electromagnetic section of the calorimeter. A cosmic ray traversing the CDF detector can deposit energy in the calorimeter without registering a track in the tracking detectors. If the beam halo background events and cosmic ray background events, as described above, do not overlap with beam crossing events that produce hard $p\bar{p}$ collisions, then there will be little activity in the tracking detectors. Therefore, by requiring $F_{\mathrm{ch}} > 0.1$ we reject backgrounds that have little tracking activity. More detailed explanations of these two variables and how they reduce the non-$p\bar{p}$ collision events are described in [25]. We also reject events if the reconstruction cone of any jet in the event enters an uninstrumented region of the calorimeter.

III. BACKGROUND SOURCES AND EVENT SELECTION

The dominant backgrounds to the stop and sbottom searches in the jets and $\not\!\!E_T$ signature are production of multijet, W or Z boson with jets, single top, $t\bar{t}$, and di-boson ($WW/WZ/ZZ$) final states. We use the ALPGEN generator to simulate the W and Z boson plus parton production, with HERWIG used to model parton showers [26,27]. Multijet, top quark, and di-boson production are simulated with PYTHIA [28]. All the Monte Carlo (MC) SM background samples were generated using the CTEQ5L PDFs [29]. In generating the multijet sample, we select events where there are b or c outgoing partons/hadrons in the final state [heavy-flavor (HF) multijet]. To normalize the SM top background samples, we use the NLO cross section values for single top and $t\bar{t}$ production [30–32]. We use the MCFM program to obtain the NLO cross sections for W/Z + jets and di-boson production [33,34]. The HF multijet sample is normalized using kinematic regions in the data that are dominated by multijet production. In multijet production events, the $\not\!\!E_T$ is usually due to jet energy mismeasurement. In this case the $\vec{\not\!\!E}_T$ tends to point in the same direction as the jet whose energy is mismeasured. In the $\not\!\!E_T$ + jets data sample used in this analysis, the events at higher $\not\!\!E_T$ are dominated by non-multijet SM contributions. Therefore, the multijet dominant kinematic regions are low $\not\!\!E_T$ regions ($50 < \not\!\!E_T < 70$ GeV), and regions where a jet is aligned in the direction of $\not\!\!E_T$. We obtain an average normalization factor $k_{\mathrm{HFmultijet}} = 1.46 \pm 0.37$ where the uncertainty is mainly due to the uncertainty from jet energy calibration and resolution [24]. The $k_{\mathrm{HFmultijet}}$ factor is used to normalize the HF multijet sample to estimate the HF multijet contribution in the signal region.

Data selection is optimized by maximizing the statistical significance of a simulated stop/sbottom signal over the expected background events in the data. The optimization is performed prior to examining the signal regions of the data. As the signal production cross section and event kinematics (for example jet E_T, $\not\!\!E_T$) could vary significantly across stop and sbottom masses, we determine separate sets of optimized cuts for three mass ranges. The "low," "medium," and "high" mass ranges used for the stop (sbottom) search are $m_{\tilde{t}_1} < 100$ GeV/c^2, $100 \le m_{\tilde{t}_1} < 120$ GeV/c^2, and $m_{\tilde{t}_1} \ge 120$ GeV/c^2 ($m_{\tilde{b}_1} < 140$ GeV/c^2, $140 \le m_{\tilde{b}_1} < 180$ GeV/c^2, and $m_{\tilde{b}_1} \ge 180$ GeV/c^2). The selection cuts for the stop and sbottom are summarized in Tables I and II respectively. At the initial stage of event selection, the data sample is dominated by multijet background events. We employ several selection cuts to minimize their contribution. To reduce multijet background and avoid regions where the $\not\!\!E_T$ trigger is inefficient, we require $\not\!\!E_T > 50$ GeV. The $\not\!\!E_T$ trigger is ~75% efficient in this region. Next we require

TABLE I. The event selection cuts for pair production of stop in the low, medium, and high stop mass regions. Jet1, Jet2, and Jet3 are, respectively, the first, second, and third leading jets. The cuts that are listed only under the medium column are common for all three mass ranges.

Mass range (GeV/c^2)	Low	Medium	High
	<100	100–120	>120
$\not\!\!E_T$ (GeV)	>50	>50	>50
E_T Jet1 (GeV)	>35	>45	>55
E_T Jet2 (GeV)	>15	>15	>25
E_T Jet5 (GeV)	>15	>15	>15
$\mid \eta \mid$: Jet1, Jet2, Jet3	$\mid \eta_1 \mid <1.2, \mid \eta_2 \mid <1.5, \mid \eta_3 \mid <2.0$		
Veto additional jets	$E_T > 8$ GeV, $2< \mid \eta \mid <3.6$		
$\Delta\phi$(Jet1, Jet2) accepted range (deg)	70–160	70–160	70–160
$\Delta\phi$(Jet, $\not\!\!E_T$) accepted range (deg)	45–180	45–180	45–180
E_T(Jet2) + $\not\!\!E_T$ (GeV)	>65	>85	>105
$E^{\nu}_{T_{J12MET}}$ (GeV)	<15	<15	<15
Lepton Veto	YES	YES	YES
minimum # tracks in jet ($\mid \eta \mid <1$)	4	4	4
JET-PROBABILITY Tagging	$>= 1$ tag (JP $< 5\%$)		

that there be only two or three reconstructed jets in $|\eta| < 2$. Events with any additional jets with $E_T > 8$ GeV and $2 < |\eta| < 3.6$ are rejected. Most of the time the two highest-E_T jets in multijet events are antiparallel. However, this is not the case in the stop (sbottom) pair production since the c (b) jet recoils against the $\tilde{\chi}_1^0$ in the stop (sbottom) decay. Therefore, we require that the opening angle between the two highest E_T jets be less than 160 degrees in the plane perpendicular to the beam. The large $\not\!\!E_T$ in multijet events that survive the earlier cuts is usually due to jet energy mismeasurement. Thus, to further reduce this background we require a minimum azimuthal separation between the direction of the jets and $\vec{\not\!\!E}_T$ of $\Delta\phi(\text{Jet}, \not\!\!E_T) > 45°$. For multijet events that pass the minimum azimuthal separation requirement, but have large $\not\!\!E_T$ due to jet energy mismeasurement, the magnitudes of the $\not\!\!E_T$ and the second leading jet's transverse energy are often anticorrelated. Therefore, we require the sum E_T(Jet2) + $\not\!\!E_T$ to be above the values listed in Tables I and II.

In stop (sbottom) pair production, where each stop (sbottom) decays into a charm (bottom) quark and a neutralino, the vector sum of the transverse energy of the two c jets (b jets) should balance against the missing transverse energy from the escaping neutralinos. We explore the correlation between the missing transverse energy and the transverse energy of the first and second leading jets

TABLE II. The event selection cuts for pair production of sbottom in the low, medium, and high sbottom mass regions. Jet1, Jet2, and Jet3 are, respectively, the first, second, and third leading jets. The cuts that are listed only under the medium column are common for all three mass ranges.

Mass range (GeV/c^2)	Low	Medium	High
	<140	140–180	>180
$\not\!\!E_T$(GeV)	>50	>55	>65
E_T Jet1 (GeV)	>35	>55	>75
E_T Jet2 (GeV)	>15	>15	>35
E_T Jet3 (GeV)	>15	>15	>15
$\mid \eta \mid$: Jet1, Jet2, Jet3	$\mid \eta_1 \mid <1.2, \mid \eta_2 \mid <1.5, \mid \eta_3 \mid <2.0$		
Veto additional jets	$E_T > 8$ GeV, $2< \mid \eta \mid <3.6$		
$\Delta\phi$(Jet1, Jet2) accepted range (deg)	60–160	50–160	40–160
$\Delta\phi$(Jet, $\not\!\!E_T$) accepted range (deg)	45–180	45–180	45–180
E_T(Jet2) + $\not\!\!E_T$ (GeV)	>80	>120	>160
$E^{\nu}_{T_{J12MET}}$ (GeV)	<15	<15	<15
Lepton Veto	YES	YES	YES
minimum # tracks in jet ($\mid \eta \mid <1$)	4	4	4
JET-PROBABILITY Tagging	$>= 1$ tag (JP $< 1\%$)		

through the variable $E^{\nu}_{T_{J12MET}}$, which is defined as

$$E^{\nu}_{T_{J12MET}} = (\vec{E}_{T_{J1}} + \vec{E}_{T_{J2}} + \vec{\not{E}}_T) \cdot \left(\frac{\vec{E}_{T_{J1}} + \vec{E}_{T_{J2}}}{|\vec{E}_{T_{J1}} + \vec{E}_{T_{J2}}|} \right). \quad (1)$$

$\vec{E}_{T_{J1}}$ and $\vec{E}_{T_{J2}}$ are, respectively, the vectors of the transverse energy of the first and second leading jets. For pair production of stop (sbottom), $E^{\nu}_{T_{J12MET}}$ is expected to be insignificant, i.e. within the calorimeter jet energy resolution. For multijet production, due to its high jet multiplicity, the missing transverse energy caused by the mismeasurement of a single jet's energy, may not balance against the transverse energy of the first and second leading jets. In top quark pair production, the missing transverse energy caused by the escaping neutrino in the W boson decay also does not necessarily balance against the first and second leading jets in the event. Therefore, $E^{\nu}_{T_{J12MET}}$ is large in these background events. To reduce the contribution from top quark production, and to further reduce multijet background, we require $E^{\nu}_{T_{J12MET}} < 15$ GeV for both stop and sbottom analyses.

To reduce the background contribution from W/Z + jets and top quark production, we reject events with one or more identified leptons. Candidate electrons must have a track associated with a cluster in the electromagnetic calorimeter with $E_T > 10$ GeV. Its electromagnetic to hadronic energy ratio and shower profile must also be consistent with that expected for electrons. Candidate muons are identified as tracks with $p_T > 10$ GeV/c that extrapolate to hits in the muon chambers and to energy deposited in the calorimeters consistent with a minimum ionizing particle. To increase lepton detection efficiency, candidate leptons (electrons, muons, taus) are also identified by isolated tracks with $p_T > 10$ GeV/c. The number of tracks associated with the first and second leading jets should be four or more. This selection reduces contributions from W + jets and Z + jets in which the gauge bosons decay into tau leptons.

For the stop and sbottom search, the signal contains a large fraction of heavy-flavor jets compared to the SM background, which is dominated by light-flavor jets. To enhance the signal over SM background, we identify the heavy-flavor jets using the JET-PROBABILITY (JP) algorithm [35]. Jets from heavy-flavor partons are characterized by secondary decays that are displaced from the primary vertex; thus their tracks have a large impact parameter. Light-flavor jets appear to come from the primary interaction and their tracks' impact parameters are consistent with the primary vertex (within the resolution of the tracking detector). The JP algorithm examines the impact parameter of each track from a candidate jet and computes a probability that the jet is a light/heavy jet. Jets from the primary (secondary) vertex are assigned a large (small) JP value. For the stop (sbottom) search at least one jet was required to have a JP $< 5\%$ (JP $< 1\%$). A looser cut is used to tag c jets as their lifetime is shorter compared to b jets. The efficiency to tag a fiducial c or b jet increases with the transverse energy of the jet, and plateaus at $E_T \sim 80$ GeV. The average efficiency to tag a fiducial c jet (b jet) with JP value of JP $< 5\%$ (JP $< 1\%$) is $\sim$17% ($\sim$ 40%) [35].

Light-Flavor Background

A significant source of background is that due to misidentification of light-flavor jets as heavy flavor. In this case one or more light-flavor jets are tagged as a c jet or b jet by the JP algorithm (mistag). A detailed description of the mistag rate is given in [35]. Here we provide a brief summary of its measurement and how it is applied in the stop and sbottom searches. The mistag rate is measured in inclusive jet samples. The rate of misidentifying a light-flavor jet as a heavy-flavor jet is about $\sim$1% ($\sim$ 5%) for tagging at JP $< 1\%$ (JP $< 5\%$). Uncertainties on the mistag rates are due to uncertainties in the contribution of long-lived Λ's and K's in the light-flavor jets and uncertainties in the effect of particle interactions in the detector materials; these relative uncertainties are 9% for JP $< 1\%$, and 13% for JP $< 5\%$. An additional relative uncertainty on the

TABLE III. The number of observed data events, and the number of expected events from standard model sources in the stop signal region. The first uncertainty is from limited simulation statistics and the second is from systematic uncertainties.

Mass range (GeV/c^2)	Low	Medium	High
	<100	100–120	>120
Process		Events expected	
W + jets	11.5 ± 2.4 ± 2.6	9.3 ± 2.3 ± 2.1	4.0 ± 1.5 ± 0.9
Z + jets	9.9 ± 0.5 ± 2.0	7.3 ± 0.4 ± 1.5	4.1 ± 0.3 ± 0.8
Di-boson	2.5 ± 0.1 ± 0.5	2.0 ± 0.1 ± 0.4	0.9 ± 0.1 ± 0.2
Top	5.2 ± 0.2 ± 0.8	4.9 ± 0.2 ± 0.8	3.9 ± 0.2 ± 0.6
HF Multijet	32.5 ± 5.2 ± 8.1	17.9 ± 4.0 ± 4.5	2.6 ± 1.5 ± 0.6
Mistag	75.4 ± 2.2 ± 10.7	53.5 ± 2.0 ± 7.6	27.2 ± 1.5 ± 3.9
Total Expected	137 ± 6.2 ± 14.6	94.9 ± 5.0 ± 9.9	42.7 ± 2.6 ± 4.6
Data	151	108	43

TABLE IV. The number of observed data events, and the number of expected events from standard model sources in the sbottom signal region. The first uncertainty is from limited simulation statistics and the second is from systematic uncertainties. The contribution from diboson background is found to be negligible in the sbottom search.

Mass range (GeV/c^2)	Low	Medium	High
	<140	140–180	>180
Process		Events expected	
W + jets	$5.5 \pm 1.2 \pm 1.2$	$1.5 \pm 0.6 \pm 0.3$	$0.5 \pm 0.4 \pm 0.1$
Z + jets	$6.0 \pm 0.4 \pm 1.1$	$2.7 \pm 0.3 \pm 0.5$	$1.0 \pm 0.2 \pm 0.2$
Top	$4.2 \pm 0.2 \pm 0.6$	$2.9 \pm 0.1 \pm 0.4$	$1.2 \pm 0.1 \pm 0.2$
HF Multijet	$18.8 \pm 4.0 \pm 4.7$	$2.6 \pm 1.5 \pm 0.7$	$0^{+2.1}_{-0}$
Mistag	$20.5 \pm 0.6 \pm 2.3$	$8.1 \pm 0.5 \pm 0.9$	$2.0 \pm 0.3 \pm 0.2$
Total Expected	$55.0 \pm 4.2 \pm 5.9$	$17.8 \pm 1.7 \pm 1.6$	$4.7^{+2.1}_{-0.5} \pm 0.5$
Data	60	18	3

mistag rate of 6.7% (4.7%) for a JP cut of JP $< 1\%$ (JP $< 5\%$) is estimated by comparing the observed and predicted tag rates in different data samples [inclusive jet samples taken with different jet E_T thresholds, and high jet multiplicity (≥ 4 jets) sample]. To estimate the contribution from light-flavor background in the final data sample, we apply the measured mistag rate to the data sample, i.e. we multiply each jet by the mistag probability, after all selection cuts are applied except the heavy-flavor jet tagging. In the estimate of the heavy-flavor background contributions with MC samples, we check for the existence of a b or a c parton or hadron within a cone of $\Delta R = 0.4$ around the jet before we tag it, to avoid double counting of background events due to light-flavor jets. Since a looser tagging requirement is used to tag the c jets in the stop search than to tag the b jets in the sbottom search, we expect the stop analysis to have a larger fraction of mistag background compared to the sbottom analysis. This can be seen in Tables III and IV.

IV. DETECTION EFFICIENCY AND SYSTEMATIC UNCERTAINTIES

The total detection efficiencies for the stop and sbottom signals are estimated using the PYTHIA event generator and the CDF detector simulation program. The samples were generated using the CTEQ5L PDFs, with the renormalization and factorization scale set to the mass of the squark in the search [29]. The total stop (sbottom) signal selection efficiency in the accessible mass region varies from 0.1% to 3.4% (0.17% to 8.5%). The efficiency increases for higher stop (sbottom) mass and larger mass difference between $\tilde{t}_1$ ($\tilde{b}_1$) and $\tilde{\chi}^0_1$.

We have estimated the main contributions to the systematic uncertainty on the signal acceptance and the SM background estimation. The uncertainty due to the jet energy scale for the SM background estimation is of the order of 10%, whereas it varies from 4% to 20% for the signal efficiency, depending on the stop and sbottom masses (larger uncertainty for smaller squark mass). The systematic uncertainty from NLO cross sections in the SM background varies between 8% to 13%. The systematic uncertainty on the efficiency for tagging a c jet (b jet) is 12% (8.6%) [35]. The uncertainty on the signal acceptance due to modeling of gluon radiation from the initial-state or final-state partons is 5%. This is evaluated from signal MC samples generated with different levels of initial- and final-state radiation. The uncertainty on the signal efficiency due to the PDF choice is determined to be 2%, using the CTEQ6M uncertainty PDF set. The uncertainty from MC statistics reaches in the most selective search region 50% for the SM background, and 10% for signal. The uncertainty on the trigger efficiency is 5%, and the uncertainty on the luminosity of the data sample is 6% [36]. The quoted uncertainties are relative to the estimated signal and backgrounds.

V. RESULTS AND CONCLUSIONS

The SM contributions and the total number of observed data events are shown in Tables III and IV for the stop and sbottom searches, respectively. We find that after applying all the selection cuts, the number of observed events are consistent with the number of expected SM background events for both stop and sbottom searches. In these two searches, and for all the mass ranges, the largest source of background events is due to misidentification of light-flavor jets as c or b jets. The HF multijet background is the second largest source of SM background in the low mass range. However, its contribution is largely suppressed by the tighter cuts employed in the medium and high mass ranges.

We studied several kinematic distributions. As an example Fig. 3 shows the observed $\not\!\!E_T$ distributions from the data and the predicted $\not\!\!E_T$ distributions from the SM background for the high mass stop and medium mass sbottom searches after all selection criteria are applied. They are in good agreement with the distributions observed in the data. No evidence for stop and sbottom production is observed in any of the kinematic regions that we have studied.

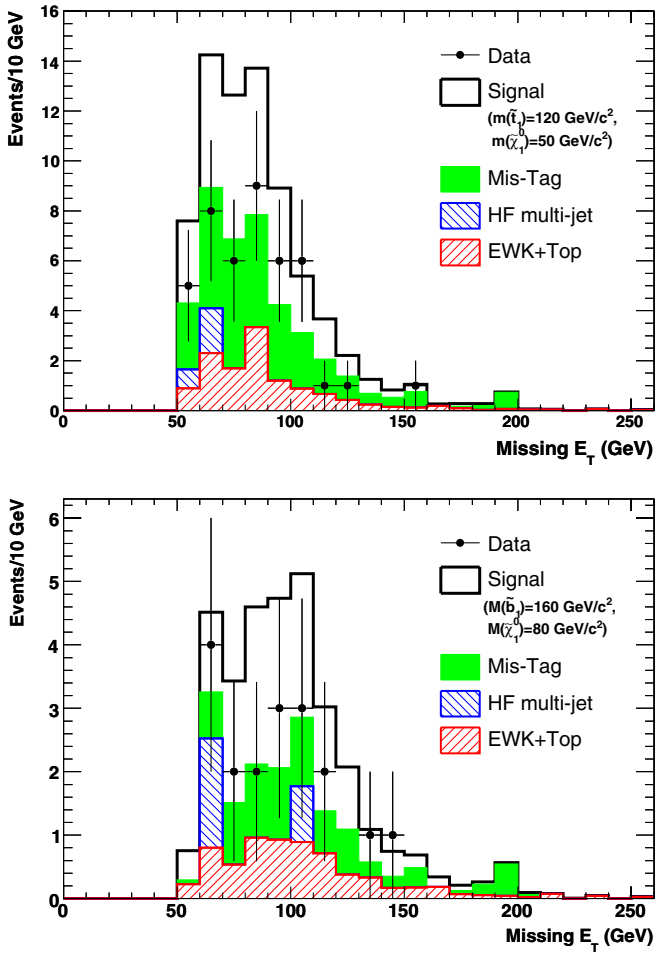

FIG. 3 (color online). The $\not\!\!E_T$ distribution in the stop (top) and sbottom (bottom) signal regions for data (solid points) compared to the SM background (filled histograms). Also shown (open histograms) are the expected distributions arising from stop pair production and decay at $m_{\tilde{t}_1} = 120\ \mathrm{GeV}/c^2$ and $m_{\tilde{\chi}_1^0} = 50\ \mathrm{GeV}/c^2$, and sbottom pair production and decay at $m_{\tilde{b}_1} = 160\ \mathrm{GeV}/c^2$ and $m_{\tilde{\chi}_1^0} = 80\ \mathrm{GeV}/c^2$.

For each of the three stop/sbottom mass ranges the number of observed events in the data is consistent with the SM expectation. An upper limit on the possible number of signal events at 95% confidence level (CL) using a modified frequentist approach [37] is calculated for each mass range. We compare this upper limit to the prediction from the NLO calculation of PROSPINO using the CTEQ6M PDFs. The uncertainties on the theoretical cross section arise from the choice of the renormalization and factorization scale and of PDFs. The changes induced by modifying Q_{rf} by a factor of 2 higher or lower than its nominal value ($Q_{\mathrm{rf}} = m_{\tilde{t}_1,\tilde{b}_1}$), and the variations observed with the CTEQ6M uncertainty PDF set, result in a change of $\sim \pm 20\%$ in the theoretical cross section, when combined in quadrature. To extract the limits on the stop and sbottom masses, we conservatively choose the one sigma lower bound of the NLO cross section associated with these uncertainties.

The interpretation of the null result in the stop search is presented as a 95% CL exclusion region in the mass plane of $m_{\tilde{\chi}_1^0}$ vs $m_{\tilde{t}_1}$, as shown in Fig. 4. The observed exclusion is smaller than the expected exclusion because we observe slightly more events in the data compared to the number of events expected from the SM processes, as shown in Table III. The maximum exclusion value of $m_{\tilde{t}_1}$ is 132 GeV/c^2 for $m_{\tilde{\chi}_1^0} = 48\ \mathrm{GeV}/c^2$, corresponding to a cross section times branching ratio limit of 2.8 pb. The maximum $m_{\tilde{\chi}_1^0}$ excluded is 57 GeV/c^2 at $m_{\tilde{t}_1} = 120\ \mathrm{GeV}/c^2$. The reach in $m_{\tilde{t}_1}$ is limited by the integrated luminosity, whereas the gap between the kinematic limit $m_{\tilde{t}_1} = m_c + m_{\tilde{\chi}_1^0}$ and the excluded region is mostly due to the $\not\!\!E_T$ requirement in the event selection.

For the sbottom search, the interpretation of the null result is presented as a 95% CL exclusion region in the mass plane of $m_{\tilde{\chi}_1^0}$ vs $m_{\tilde{b}_1}$, as shown in Fig. 5. The observed limit is larger than the expected limit at large sbottom mass because we observe fewer events than expected from the SM processes in the high sbottom mass range search. The $m_{\tilde{b}_1}$ is excluded up to 193 GeV/c^2 for $m_{\tilde{\chi}_1^0} = 40\ \mathrm{GeV}/c^2$.

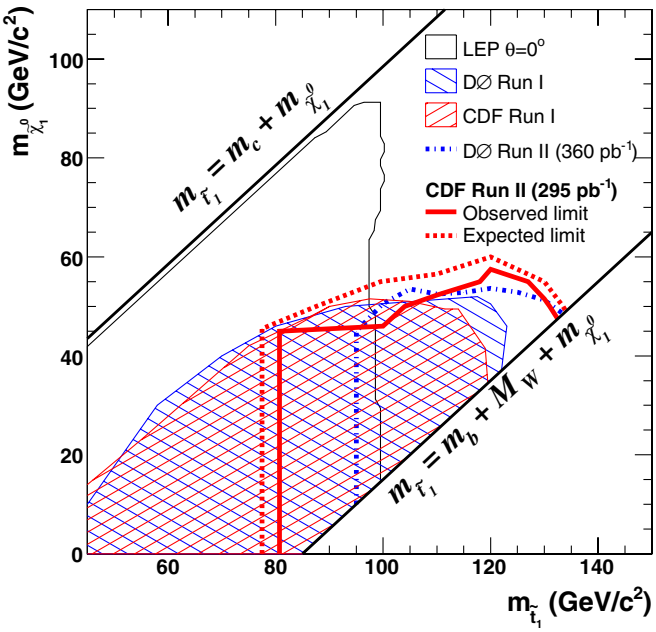

FIG. 4 (color online). The 95% CL exclusion region in the mass plane of $m_{\tilde{\chi}_1^0}$ vs $m_{\tilde{t}_1}$, assuming that stop decays exclusively into $c\tilde{\chi}_1^0$. For the region excluded by the present search (area inside the solid curve), the one sigma lower bound of the predicted NLO cross section is used to extract the mass limits. The expected exclusion contour is shown as a dashed curve. The result from the DØ Collaboration, using data from the Tevatron Run II, is presented in the same manner [16]. Results from other previous searches are also indicated [9–11]. The LEP results are presented for the case of no mixing in the stop sector ($\theta = 0°$).

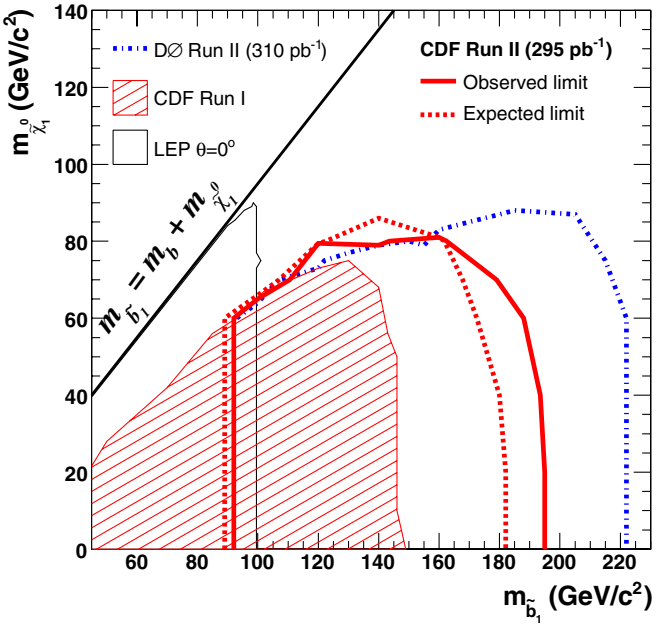

FIG. 5 (color online). The 95% CL exclusion region in the mass plane of $m_{\tilde{\chi}_1^0}$ vs $m_{\tilde{b}_1}$, assuming that sbottom decays exclusively into $b\tilde{\chi}_1^0$. For the region excluded by the present search (area inside the solid curve), the one sigma lower bound of the predicted NLO cross section is used to extract the mass limits. The dashed line indicates the expected exclusion region. The result from the D0 Collaboration, using data from the Tevatron Run II, is presented in the same manner [17]. Results from other previous searches are also indicated [9,10]. The LEP results are presented for the case of no mixing in the sbottom sector ($\theta = 0°$).

This corresponds to a cross section times branching ratio limit of 0.25 pb. The exclusion features of this plot are similar to those for the stop search.

In conclusion, we have performed searches for stop and sbottom production in proton-antiproton collisions at $\sqrt{s} = 1.96$ TeV, using 295 pb^{-1} of data recorded by the CDF experiment. In this search we assume that the stop (sbottom) decays exclusively into a c (b) quark and the lightest neutralino. The number of events that pass our selection for both stop and sbottom searches is consistent with the standard model expectation. Our 95% CL exclusion regions in the supersymmetric quark-neutralino mass plane extend beyond the LEP and the Tevtron's Run I reaches [9–11]. The exclusion reach in this stop search is comparable with D0 's latest Run II stop results [16].

ACKNOWLEDGMENTS

We thank the Fermilab staff and the technical staffs of the participating institutions for their vital contributions. This work was supported by the U.S. Department of Energy and National Science Foundation; the Italian Istituto Nazionale di Fisica Nucleare; the Ministry of Education, Culture, Sports, Science, and Technology of Japan; the Natural Sciences and Engineering Research Council of Canada; the National Science Council of the Republic of China; the Swiss National Science Foundation; the A. P. Sloan Foundation; the Bundesministerium für Bildung und Forschung, Germany; the Korean Science and Engineering Foundation and the Korean Research Foundation; the Science and Technology Facilities Council and the Royal Society, UK; the Institut National de Physique Nucleaire et Physique des Particules/CNRS; the Russian Foundation for Basic Research; the Comisión Interministerial de Ciencia y Tecnología, Spain; the European Community's Human Potential Programme; the Slovak R&D Agency; and the Academy of Finland.

[1] H. P. Nilles, Phys. Rep. **110**, 1 (1984); H. E. Haber and G. L. Kane, Phys. Rep. **117**, 75 (1985).
[2] S. P. Martin, arXiv:hep-ph/9709356.
[3] M. Quiros, Nucl. Phys. B, Proc. Suppl. **101**, 401 (2001) and references therein.
[4] P. Fayet, Phys. Lett. **69B**, 489 (1977).
[5] W. Beenakker *et al.*, Nucl. Phys. **B515**, 3 (1998).
[6] J. Pumplin *et al.*, J. High Energy Phys. 07 (2002) 012; D. Stump *et al.*, J. High Energy Phys. 10 (2003) 046.
[7] M. Drees and K. I. Hikasa, Phys. Lett. B **252**, 127 (1990); K. I. Hikasa and M. Kobayashi, Phys. Rev. D **36**, 724 (1987); J. Ellis and S. Rudaz, Phys. Lett. **128B**, 248 (1983); G. Altarelli and R. Rückl, Phys. Lett. **144B**, 126 (1984); S. Dawson, E. Eichten, and C. Quigg, Phys. Rev. D **31**, 1581 (1985); J. Ellis, G. L. Fogli, and E. Lisi, Nucl. Phys. **B393**, 3 (1993).
[8] A. Bartl, W. Majerotto, and W. Porod, Z. Phys. C **64**, 499 (1994).
[9] LEPSUSYWG Collaboration, ALEPH Collaboration, DELPHI Collaboration, L3 Collaboration, OPAL Collaboration, Report No. LEPSUSYWG/04-02.1, http://lepsusy.web.cern.ch/lepsusy/Welcome.html.
[10] T. Affolder *et al.* (CDF Collaboration), Phys. Rev. Lett. **84**, 5704 (2000).
[11] V. M. Abazov *et al.* (D0 Collaboration), Phys. Rev. Lett. **93**, 011801 (2004).
[12] T. Affolder *et al.* (CDF Collaboration), Phys. Rev. Lett. **84**, 5273 (2000); D. Acosta *et al.* (CDF Collaboration), Phys. Rev. Lett. **90**, 251801 (2003); V. M. Abazov *et al.* (D0 Collaboration), Phys. Rev. Lett. **88**, 171802 (2002); Phys. Lett. B **581**, 147 (2004).
[13] D. Acosta *et al.* (CDF Collaboration), Phys. Rev. Lett. **92**, 051803 (2004).
[14] T. Affolder *et al.* (CDF Collaboration), Phys. Rev. D **63**,

091101 (2001).
[15] A. Abulencia *et al.* (CDF Collaboration), Phys. Rev. Lett. **96**, 171802 (2006).
[16] V. M. Abazov *et al.* (D0 Collaboration), Phys. Lett. B **645**, 119 (2007).
[17] V. M. Abazov *et al.* (D0 Collaboration), Phys. Rev. Lett. **97**, 171806 (2006).
[18] D. Acosta *et al.* (CDF Collaboration), Phys. Rev. D **71**, 032001 (2005).
[19] C. S. Hill *et al.*, Nucl. Instrum. Methods Phys. Res., Sect. A **530**, 1 (2004); A. Sill *et al.*, Nucl. Instrum. Methods Phys. Res., Sect. A **447**, 1 (2000); T. Affolder *et al.*, Nucl. Instrum. Methods Phys. Res., Sect. A **453**, 84 (2000).
[20] T. Affolder *et al.*, Nucl. Instrum. Methods Phys. Res., Sect. A **526**, 249 (2004).
[21] CDF uses a cylindrical coordinate system in which θ is the polar angle to the proton beam, ϕ is the azimuthal angle about the beam axis, and pseudorapidity is defined as $\eta = -\ln\tan(\theta/2)$. The transverse energy and transverse momentum are defined as $E_T = E\sin\theta$ and $p_T = p\sin\theta$, where E is energy measured in the calorimeter and p is momentum measured by the tracking system. The missing transverse energy vector, $\vec{\not\!\!E}_T$, is $-\sum_i E_T^i \boldsymbol{n}_i$, where $\boldsymbol{n}_i$ is the unit vector in the azimuthal plane that points from the beamline to the ith calorimeter tower. The scalar quantity $\not\!\!E_T$ is the magnitude of the vector $\vec{\not\!\!E}_T$.
[22] L. Balka *et al.*, Nucl. Instrum. Methods Phys. Res., Sect. A **267**, 272 (1988); S. Bertolucci *et al.*, Nucl. Instrum. Methods Phys. Res., Sect. A **267**, 301 (1988); M. Albrow *et al.*, Nucl. Instrum. Methods Phys. Res., Sect. A **480**, 524 (2002).
[23] F. Abe *et al.* (CDF Collaboration), Phys. Rev. D **45**, 1448 (1992).
[24] A. Bhatti *et al.*, Nucl. Instrum. Methods Phys. Res., Sect. A **566**, 375 (2006).
[25] T. Affolder *et al.* (CDF Collaboration), Phys. Rev. Lett. **88**, 041801 (2002).
[26] M. L. Mangano *et al.*, J. High Energy Phys. 07 (2003) 001. We use version 1.2.
[27] G. Corcella *et al.*, J. High Energy Phys. 01 (2001) 010; arXiv:hep-ph/0210213. We use version 6.4a.
[28] T. Sjostrand, P. Eden, C. Friberg, L. Lonnblad, G. Miu, S. Mrenna, and E. Norrbin, Comput. Phys. Commun. **135**, 238 (2001).
[29] H. L. Lai *et al.* (CTEQ Collaboration), Eur. Phys. J. C **12**, 375 (2000).
[30] M. Cacciari *et al.*, J. High Energy Phys. 04 (2004) 068.
[31] B. W. Harris, E. Laenen, L. Phaf, Z. Sullivan, and S. Weinzierl, Phys. Rev. D **66**, 054024 (2002).
[32] Z. Sullivan, Phys. Rev. D **70**, 114012 (2004).
[33] J. M. Campbell and R. K. Ellis, Phys. Rev. D **60**, 113006 (1999).
[34] J. M. Campbell and R. K. Ellis, Phys. Rev. D **65**, 113007 (2002).
[35] A. Abulencia *et al.* (CDF Collaboration), Phys. Rev. D **74**, 072006 (2006).
[36] S. Klimenko, J. Konigsberg, and T. Liss, Report No. FERMILAB-FN-0741, 2003; D. Acosta *et al.*, Nucl. Instrum. Methods Phys. Res., Sect. A **494**, 57 (2002).
[37] T. Junk, Nucl. Instrum. Methods Phys. Res., Sect. A **434**, 435 (1999).